Biophysical Chemistry 40 (1991) 97–108
Elsevier Science Publishers B.V., Amsterdam

BIOCHE 01558

Characterization of proline-containing right-handed α-helix by molecular dynamics studies

R. Sankararamakrishnan, N. Sreerama * and Saraswathi Vishveshwara **

Molecular Bio-Physics Unit, Indian Institute of Science, Bangalore 560 012, India

Received 17 July 1990
Revised manuscript received 20 October 1990
Accepted 8 November 1990

Proline-containing right-handed α-helix; Molecular dynamics; Helix bend; Average structural parameters

Proline residues play a special role in shaping the secondary and tertiary structures of proteins. Many of these aspects have been studied in great detail. Current interest lies in elucidating the structure of right-handed α-helical fragments which contain proline in the middle of the helix. Such structures play an important role in membrane proteins and in the tight packing of globular proteins. Analysis of several crystal structures and energy minimization using flexible geometry have elucidated the nature of the bend produced by proline in the right-handed α-helical structure. Molecular dynamics (MD) simulation studies are ideally suited to characterize rigidity or flexibility in different parts of the molecule and can also give an idea of various conformations of the molecule which can exist at a given temperature. Hence, MD studies on Ace-$(Ala)_6$-Pro-$(Ala)_3$-NHMe have been carried out for 100 ps after equilibration and the resulting trajectories have been analyzed. Information regarding the average values, r.m.s. fluctuations of internal parameters and the time spent in different conformations are discussed. Energy minimization has been carried out on selected MD simulated points in order to analyze the characteristics of different conformations.

1. Introduction

The proline residue is known to play an important role in the structure of proteins [1–5]. Recently, the focus has been on understanding the role of proline residues which are present in the middle of right-handed α-helices [6–8]. A bend in the helix axis of about 20–30° introduced by proline in right-handed α-helices on the surface of globular proteins may be important in tight packing of the molecule. Also, a number of membrane proteins such as bacteriorhodopsin and acetylcholine receptor [9] have helical segments passing through the membrane and the proline residues in those segments are known to affect the activity of these proteins considerably [10–15]. The exact role of proline is not very clear and some attempts to characterize proline-containing helices by crystal structure analysis [6–8], ^{1}H-NMR studies [16] and energy minimization [6,8] have been made. From our previous studies using energy-minimization techniques combined with crystal structure analysis [7], a set of geometrical parameters characterizing the bend due to proline in the right-handed α-helix was provided. These studies were based on a limited number of crystal structures that were available and information regarding deviations from the average values could not be obtained. Molecular dynamics (MD) studies are ideally suited to characterize the rigidity or flexibility of different parts of a molecule. Average parameters can also be obtained along with r.m.s. deviations. Hence, in the present paper, Ace-$(Ala)_6$-Pro-$(Ala)_3$-NHMe has been characterized by MD

* Present address: Department of Biochemistry, Colorado State University, Fort Collins, CO 80523, USA.
** To whom correspondence should be addressed.

0301-4622/91/$03.50

studies. Selected points obtained during the MD simulation were further subjected to energy-minimization investigation in order to obtain more information on the structural parameters, global minimum and the relation between various local minima.

2. Methods

MD simulations on Ace-$(Ala)_6$-Pro-$(Ala)_3$-NHMe were performed using the program AMBER [17,18] which was adapted to run on DEC-1090 and IBM PC/AT compatible machines. The internal parameters for the starting structure for Ace-$(Ala)_6$-Pro-$(Ala)_3$-NHMe were taken from ref. 7 and the energy was minimized using the AMBER minimization module until the r.m.s. gradient of the energy was less than 0.1 kcal/mol. The structure thus obtained was taken as the starting structure for the MD simulation. Initially, random velocities were assigned to each atom using the Maxwellian distribution. The system was equilibrated to 300 K over a period of 25 ps. The average properties of the system, such as kinetic energy, remained constant at the end of equilibration. The simulation was continued for another 100 ps. The AMBER potential energy function has the following form

$$E_{\text{total}} = \sum_{\text{bonds}} K_b(R - R_0)^2 + \sum_{\text{angles}} K_a(\theta - \theta_0)^2 + \sum_{\text{dihedrals}} K_d/2[1 + \cos(n\phi - \gamma)] + \sum_{\substack{i<j \\ \text{non-bonded}}} \left[B_{ij}/r_{ij}^{12} - A_{ij}/r_{ij}^{6} + q_i q_j/\epsilon_{ij} r_{ij}\right] + \sum_{\text{H-bonds}} \left[C_{ij}/r_{ij}^{12} - D_{ij}/r_{ij}^{10}\right]$$

The above energy function includes the harmonic bond stretching, bond angle bending and a truncated Fourier series for torsion angles as its first three terms. The fourth term sums the standard Lennard-Jones and electrostatic terms for non-bonded interactions. The final term calculates the energy due to hydrogen bonding. Values for parameters (K_a, θ_0, K_b, R_0, K_d, γ, A_{ij}, B_{ij}, C_{ij} and D_{ij}) in the potential function have been reported [19,20]. The AMBER MD program uses a Verlet leapfrog algorithm [21]. A time step of 0.001 ps was chosen. All hydrogen atoms were explicitly included and hence the force field corresponding to an all-atom model [20] was used. All bonds involving hydrogen atoms were constrained using the algorithm SHAKE. The simulation was performed in vacuum and a distance-dependent dielectric constant was used. The output from the MD run contained a total of 1000 'snapshots' of the atomic coordinates during the 100 ps evolution time with each snapshot taken at 0.1-ps intervals.

Except for the virtual torsional angles (VTs), the averages of all other parameters and the r.m.s. fluctuations were obtained using the AMBER MD analysis program. The notation of the parameters is shown in fig. 1. For consistency the same notation as was previously used has been followed [7]. In addition to bond angles, dihedral angles and hydrogen bonds, the virtual torsional angles of C^α atoms were also analyzed. The notation VT_i represents the virtual torsional angle C_i^α-C_{i+1}^α-C_{i+2}^α-C_{i+3}^α where C_i^α is the C^α carbon atom of the i-th residue in the 10-residue fragment (the terminal residues Ace and NHMe have not been included). The average values and the r.m.s. fluctuations of all the virtual torsional angles were obtained by a separate program written for the IBM PC/AT, which was also used to obtain the trajectories presented in figs 2–5. In our previous study [7], the virtual torsional angle C_{p-3}^α-C_{p-2}^α-C_{p-1}^α-C_p^α (VT_4, designated as ρ) showed a greater deviation from the average value of an idealized α-helix. Hence, this parameter has been investigated in detail.

11 structures from the 100 ps MD simulation were submitted to energy-minimization procedures. These structures lie in the range 75–85 ps. The proline *up* and *down* conformations were observed equally in these 11 structures and the virtual torsional angle VT_4 ranged from 50 to 75°. Using the AMBER minimization module these structures were first minimized by the steepest descent method followed by the conjugate gradient method. The steepest descent method was used for the first 50 cycles and then the conjugate gradient method was followed until convergence was obtained. The resulting structures were fur-

ther minimized by the Newton-Raphson (NR) minimization method using the AMBER NMODE module. The conformational parameters and the hydrogen bonds were analyzed and compared at all three stages.

3. Results and discussion

The analyses of the MD simulations were carried out in order to elucidate the nature of the flexibility and rigidity exhibited by various parts of the right-handed α-helix due to the presence of a proline residue. This was carried out by (1) analyzing the average structural parameters as well as (2) by examining the results of some energy-minimized structures. The analysis of the average parameters was divided into three sections: (a) the internal parameters of right-handed α-helices containing proline, (b) the characterization of the bend introduced by proline in terms of virtual torsional angles and hydrogen bonds and (c) the nature of proline puckering in the right-handed α-helix.

3.1. Analysis of average structural parameters

3.1.1. Backbone internal parameters

In a standard right-handed α-helix the internal parameters such as the bond angles and the dihedral angles, ϕ and ψ, remain more or less constant (idealized theoretical values give $\phi = -57.5°$ and $\psi = -47.5°$ [22]; average values obtained from crystal structures show $\phi = -63.8°$ (± 6.6) and $\psi = -41.0°$ (± 7.2) [23]). In the present study on proline-containing helix, the average values of these parameters over a period of 100 ps are obtained by MD simulations. These values obtained for the bond angles and dihedral angles along with the r.m.s. fluctuations for Ace-$(Ala)_6$-Pro-$(Ala)_3$-NHMe are listed in table 1. The trajectories of ϕ and ψ in the proline region are presented in fig. 2a and b. It may be noted that the bond angles θ^2_{p-1} and θ^3_{p-1} are wider by about 2° compared to those reported for a standard α-helix. Among the dihedral angles, the maximum deviation from the standard α-helix is seen in the parameters ϕ_{p-1} and ψ_{p-1}. The simulated values of these dihedral angles correspond to the goniometric helix [24]. Deviations are also obtained in the parameters ranging from ϕ_{p-4} to ψ_p. The values of ϕ_{p-3} and ϕ_{p-2} are more negative and the values of ψ_{p-3} and ψ_{p-2} are generally less negative than the standard values. The deviations in the parameters discussed above due to the presence of proline were also indicated by the crystal structure averages and their minimized structures. Whereas the crystal structure analysis was based on only a few available data, the present MD analysis is an average obtained over a large number of simulation points. Further, the r.m.s. fluctuations reported in table 1 can be useful in establishing the range of values which these parameters can take at a temperature of about 300 K.

3.1.2. Bend characterizing parameters

Previous studies [7] have shown that the virtual torsional angle (C^α_{p-3}-C^α_{p-2}-C^α_{p-1}-C^α_p) deviates from the standard α-helical value ($\simeq 50°$) due to

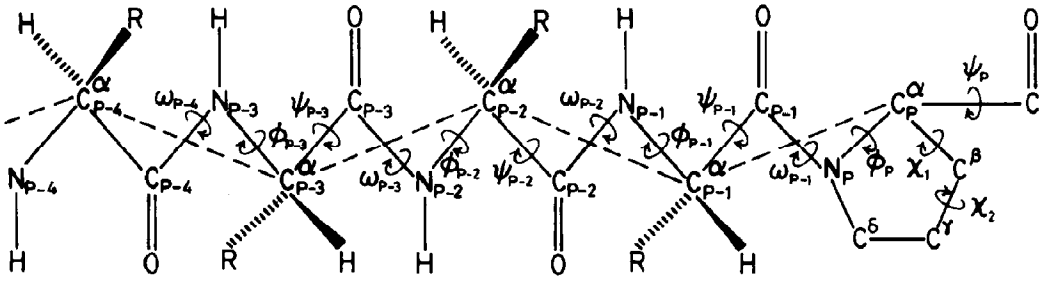

Fig. 1. Conformational parameters of poly(L-Ala) containing a proline residue in the middle. 'R' represents the alanine residue. The virtual bonds between C^α atoms are represented by dashed lines. Details of the virtual torsional angles are explained in the text. The bond angles C'_{p-1}-N_p-C^α_p, N_p-C^α_p-C'_p and C^α_p-C'_p-N_{p+1} are denoted as θ^1_p, θ^2_p and θ^3_p, respectively. The other bond angles follow similar notation.

the presence of proline. The MD trajectories of the virtual torsional angles are shown in fig. 3 and the average values with r.m.s. flucutations are given in table 2a. VT_1 and VT_7 correspond to the beginning and the end of the helix, respectively. VT_4 ($\rho = 63.9°$) exhibits the maximum deviation from the standard α-helical value and the r.m.s. fluctuation (12.9°) is also the highest in this case. The VT_4 value varies from 40 to 90° with an average around 64°, similar to the range of values observed in the crystal structures. Further, although the average value of VT_4 is around 64°, it continuously changes from about 50 to 80°, with the period of oscillation being about 2–4 ps throughout the 100 ps simulation. This suggests that the helix will be oscillating continuously between an almost straight and a largely bent structure and the bend observed in the crystal structures could very well be an averaged one.

An analysis of the hydrogen bonds in the region of the proline residue also gives an idea of the nature of bend. The mean and the r.m.s. fluctuations are given in table 2b and the trajectories of the hydrogen bonds which are affected during the simulation are depicted in fig. 4. Due to the lack of the amide proton on proline, the hydrogen bond $N_p \cdots O_{p-4}$ is absent. According to previous crystal structure analysis and energy-minimization studies [7], the hydrogen bond between N_{p+1} and O_{p-3} is also absent. However, the MD trajectory now reveals that this hydrogen bond is not broken all the time. The system seems to oscillate between a hydrogen-bonded structure ($O \cdots H \simeq 1.9$ A°) and a non-hydrogen-bonded structure ($O \cdots H \simeq 3.8$ A°). The period of oscillation is about 2–4 ps and the trajectory resembles very much that of VT_4 (fig. 3). This further supports the suggestion that the system may be oscil-

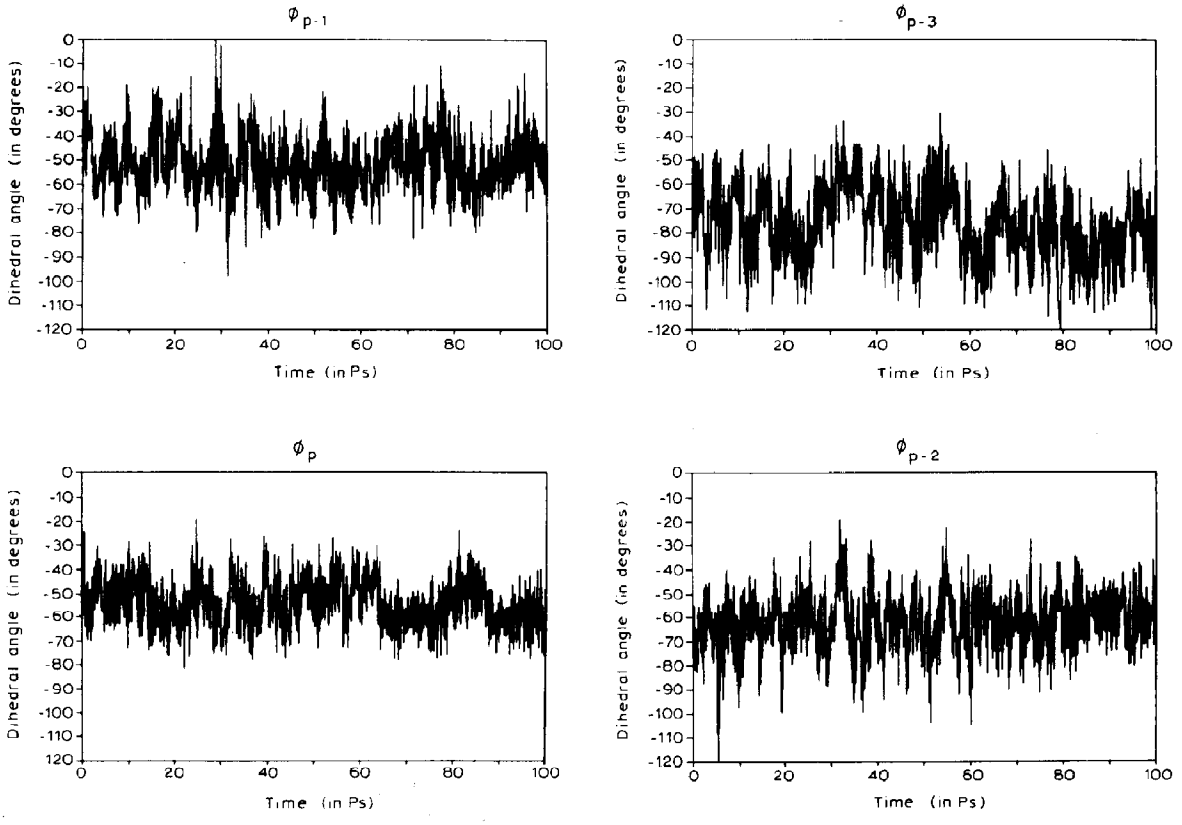

Fig. 2a. MD trajectories of the dihedral angles ϕ.

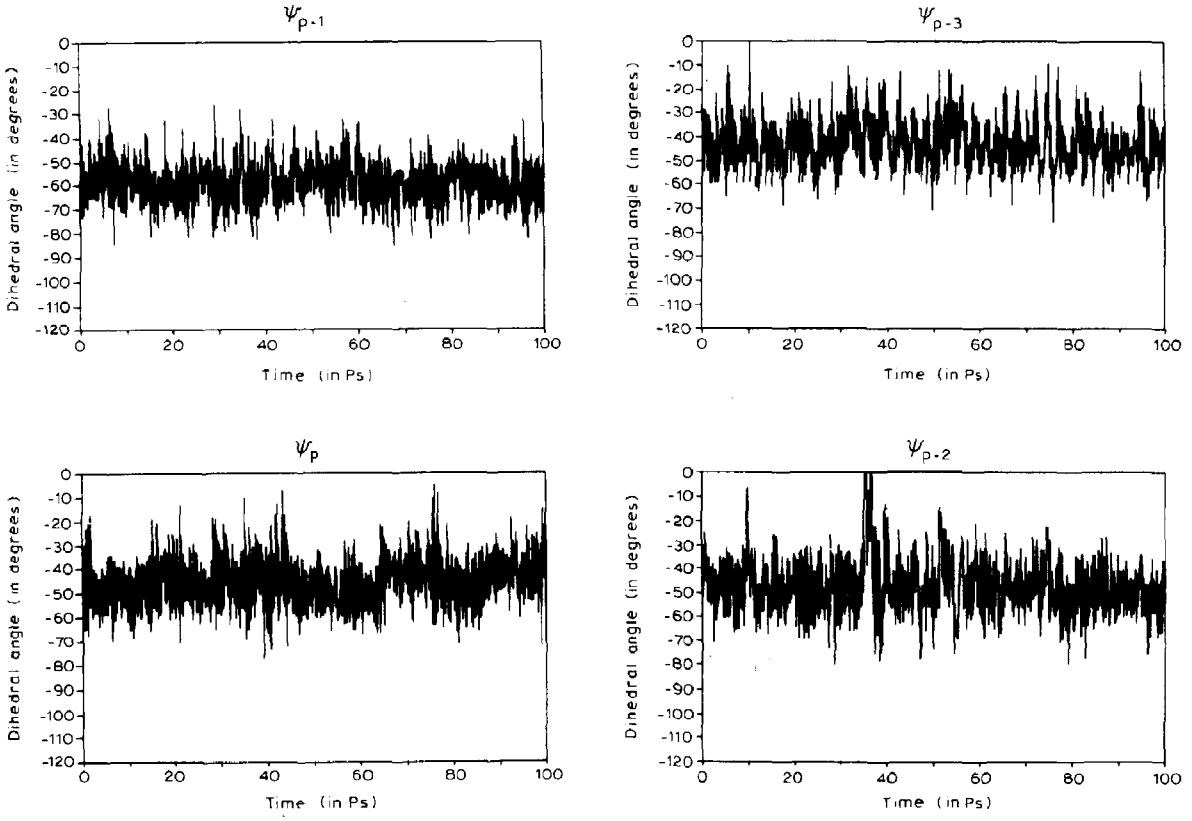

Fig. 2b. MD trajectories of the dihedral angles ψ.

lating between an almost straight helix with the $N_{p+1} \cdots O_{p-3}$ hydrogen bond, to a highly bent structure in which the $N_{p+1} \cdots O_{p-3}$ distance is about 4.8 A°.

Apart from the nature of the bend mentioned above, the MD analysis in the region of 30–60 ps also shows other structural variations. VT_3 is around the average value in the regions 0–30 and 60–100 ps whereas it shows a large variation, similar to that discussed for VT_4, in the region 30–60 ps. Similarly, the hydrogen bond $N_{p-1} \cdots O_{p-5}$ shows oscillatory behaviour in this region. This indicates that an isolated fragment of the size taken up for the present study undergoes other conformational change in addition to the well-characterized bend mode.

3.1.3. Proline puckering parameters

The puckering of proline can be specified by the dihedral angles χ_1 and χ_2 (fig. 1). Proline *up*, *down* and *planar* structures are observed in several crystal structures [25] containing proline in the middle of a right-handed α-helix. Previous energy minimization studies have led to either *up* or *down* conformations. From the MD trajectories of χ_1 and χ_2 (fig. 5), it is clear that whenever χ_1 is positive, χ_2 is negative and vice versa. This anti-correlation behaviour is also evident from the

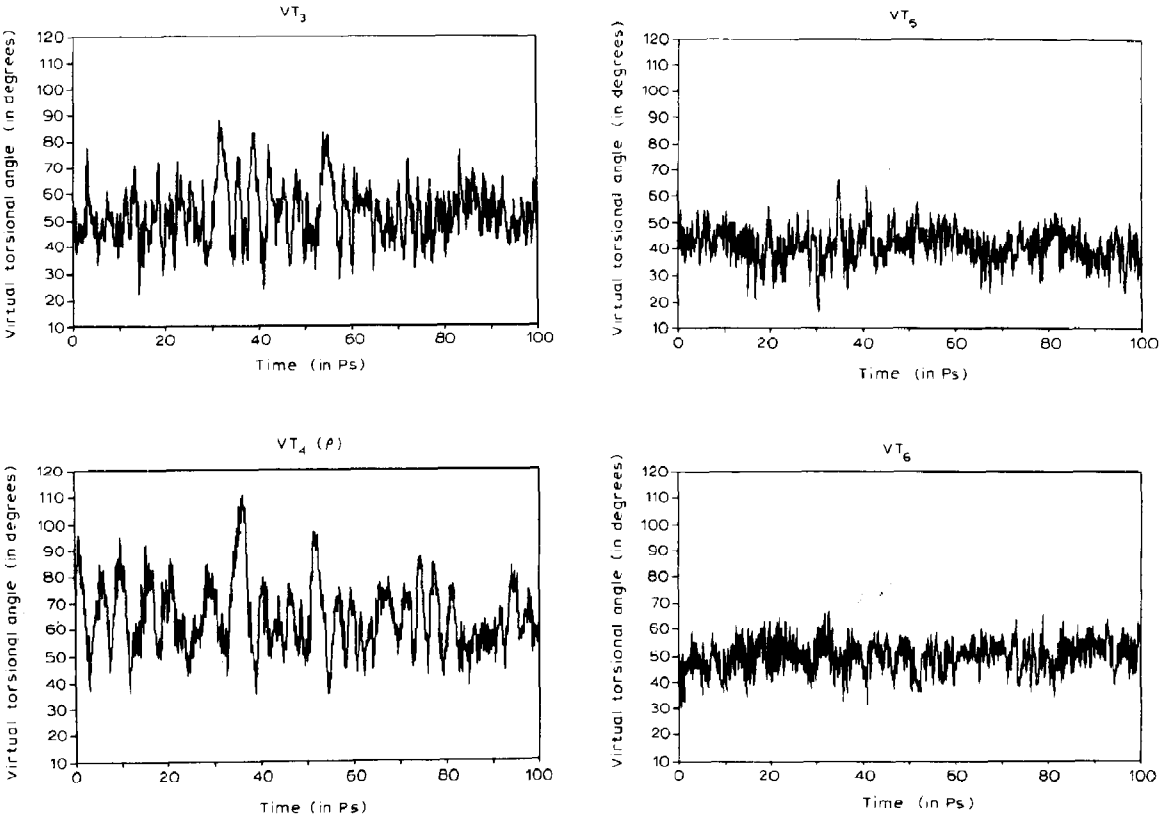

Fig. 3. MD trajectories of the virtual torsional angles.

correlation coefficient which was computed to be -0.9995. Thus, the ring is either in the *up* conformation or in the *down* conformation and passes through the *planar* structure ($\chi_1 = \chi_2 = 0.0$) only during the transition from one puckered state to another. The two structures fluctuate with a period ranging from 2 to 20 ps. The average values of χ_1 and χ_2 are -4.2 and $2.8°$, respectively, during the 100 ps simulation and the r.m.s. fluctuations are ± 25.2 and $\pm 32.3°$ corresponding to χ_1 and χ_2, respectively. The *planar* conformation which has been observed in some crystal structures may be due to an average of the *up* and *down* structures. Although the energies of the two proline structures are very much the same, they lead to small differences in the internal parameters of the helix. Such parameters were extracted by averaging the values obtained in the region 45–65 ps for the *up* structure and in the region 65–80 ps for the *down* structure. The relevant parameters are given in table 3. Particularly noticeable is the parameter ω_{p-1}, which is almost planar in the *down* conformation and deviates by 7.5° from planarity in the *up* conformation. The identification of the *up* and *down* conformations was not clear from the crystal structure analysis; the dependence of ω_{p-1} on the proline puckering was also not noticed. This distinction was apparent even from previous energy-minimization studies [7]. The present MD studies, however, provide details of the average value and the range of ω_{p-1} which can be adopted for a specified proline conformation. The studies also

reveal that the parameters ϕ_{p-1}, ϕ_p and ψ_p take slightly different values depending on the proline conformation.

3.2. Energy-minimization studies

From the MD trajectories (figs 2–5) after equilibration, it is possible to identify two types of motion at 300 K. One type is related to bending of the helix, characterized by parameters such as hydrogen bonds and the virtual torsional angle (VT_4, i.e., ρ) between C^α atoms. The second type is related to the puckering of proline, and is characterized primarily by parameters such as the dihedral angles χ_1, χ_2 and ω_{p-1}. The period of oscillation is smaller for helix bending motion than for proline flipping motion. Apart from this periodic behaviour the trajectories of VT_3 and of the H-bond $N_{p-1} \cdots O_{p-5}$ also show a complicated behaviour related to the nature of the helix bend. At this point, it is not clear whether this behaviour is inherent to the proline-containing right-handed α-helix in general or is an artifact due to the short isolated segment chosen for MD studies. For this reason the minimization studies have been carried out on structures falling in the well-defined region of 75–85 ps. In this region, both proline *up* and *down* conformations were observed and the helix had gone through different phases of bending.

11 structures of Ace-$(Ala)_6$-Pro-$(Ala)_3$-NHMe obtained after dynamics simulation of 75–85 ps were submitted to further energy-minimization studies. These structures were minimized using first the steepest descent (SD) and conjugate gradient (CG) minimization procedures followed

Table 1

Average values (in °) and r.m.s. fluctuations of backbone bond angles and backbone dihedral angles during 100 ps MD simulations on Ace-$(Ala)_6$-Pro-$(Ala)_3$-NHMe

Bond angles	Average values	Dihedral angles	Average values
θ^1_{p-5}	124.1 (±3.5)	ϕ_{p-5}	−49.1 (±13.1)
θ^2_{p-5}	112.1 (±3.0)	ψ_{p-5}	−45.5 (±10.6)
θ^3_{p-5}	117.1 (±2.9)	ω_{p-5}	−179.4 (±6.9)
θ^1_{p-4}	123.3 (±3.2)	θ_{p-4}	−63.2 (±12.1)
θ^2_{p-4}	111.7 (±3.2)	ψ_{p-4}	−36.6 (±14.2)
θ^3_{p-4}	117.6 (±2.7)	ω_{p-4}	176.4 (±7.8)
θ^1_{p-3}	123.1 (±3.3)	ϕ_{p-3}	−76.8 (±16.0)
θ^2_{p-3}	110.7 (±3.4)	ψ_{p-3}	−42.7 (±10.9)
θ^3_{p-3}	117.0 (±2.8)	ω_{p-3}	−176.7 (±8.9)
θ^1_{p-2}	123.5 (±3.4)	ϕ_{p-2}	−62.4 (±13.0)
θ^2_{p-2}	111.9 (±3.2)	ψ_{p-2}	−47.1 (±12.2)
θ^3_{p-2}	117.9 (±2.9)	ω_{p-2}	−173.9 (±8.4)
θ^1_{p-1}	122.9 (±3.3)	ϕ_{p-1}	−51.0 (±12.6)
θ^2_{p-1}	113.6 (±3.2)	ψ_{p-1}	−58.8 (±9.4)
θ^3_{p-1}	120.8 (±2.7)	ω_{p-1}	175.2 (±7.8)
θ^1_p	122.3 (±2.9)	ϕ_p	−54.2 (±10.6)
θ^2_p	112.8 (±3.1)	ψ_p	−45.2 (±10.9)
θ^3_p	118.1 (±2.8)	ω_p	−179.7 (±6.8)
θ^1_{p+1}	122.2 (±3.2)	ϕ_{p+1}	−61.9 (±10.8)
θ^2_{p+1}	111.2 (±3.1)	ψ_{p+1}	−44.8 (±10.6)
θ^3_{p+1}	117.2 (±2.7)	ω_{p+1}	178.1 (±6.9)
θ^1_{p+2}	123.2 (±3.2)	ϕ_{p+2}	−64.9 (±11.5)
θ^2_{p+2}	111.2 (±3.1)	ψ_{p+2}	−43.2 (±10.9)
θ^3_{p+2}	117.4 (±2.9)	ω_{p+2}	178.5 (±8.2)

Table 2

(a) Average values (in °) and r.m.s. fluctuations of the virtual torsional angles and (b) average values and r.m.s. fluctuations of intra-helical hydrogen bond parameters during 100 ps MD simulations on Ace-$(Ala)_6$-Pro-$(Ala)_3$-NHMe

(a) Virtual torsional angle	Average values
VT_1	53.85 (±10.02)
VT_2	40.02 (±9.86)
VT_3	52.19 (±10.86)
VT_4 (ρ)	63.90 (±12.84)
VT_5	41.27 (±6.96)
VT_6	49.85 (±6.14)
VT_7	45.32 (±6.95)

(b) Description of hydrogen bonds	Distance [a] (in Å)	Angle [a] (in °)
$O_{p-7} \cdots H_{p-4}$-N_{p-4}	2.24 (±0.46)	138.1 (±20.4)
$O_{p-6} \cdots H_{p-3}$-N_{p-3}	2.39 (±0.45)	127.5 (±20.5)
$O_{p-6} \cdots H_{p-2}$-N_{p-2}	1.94 (±0.17)	159.3 (±11.7)
$O_{p-5} \cdots H_{p-1}$-N_{p-1}	2.18 (±0.56)	157.7 (±14.0)
$O_{p-3} \cdots H_{p+1}$-N_{p+1}	2.80 (±0.73)	158.3 (±10.4)
$O_{p-2} \cdots H_{p+2}$-N_{p+2}	1.92 (±0.17)	158.8 (±11.2)
$O_{p-1} \cdots H_{p+3}$-N_{p+3}	2.00 (±0.23)	157.5 (±12.4)
$O_p \cdots H_{p+4}$-N_{p+4}	2.05 (±0.39)	148.2 (±20.9)

[a] O ··· H distances and N-H ··· O angles are listed.

by the Newton-Raphson method (NR). The initial energies of all 11 structures fell within −17.0 to −30.0 kcal/mol. After SD and CG minimization the range narrowed and the energies fell between −112.0 to −117.0 kcal/mol. After NR minimization all structures minimized to the same energy (≃ −117.0 kcal/mol).

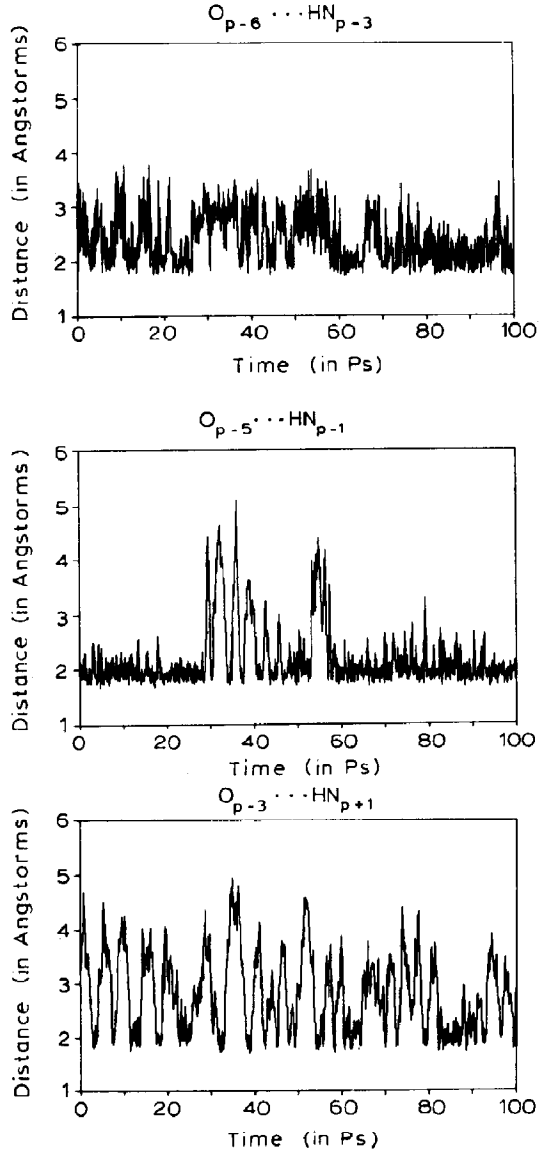

Fig. 4. MD trajectories of hydrogen bonds that are affected during the simulation.

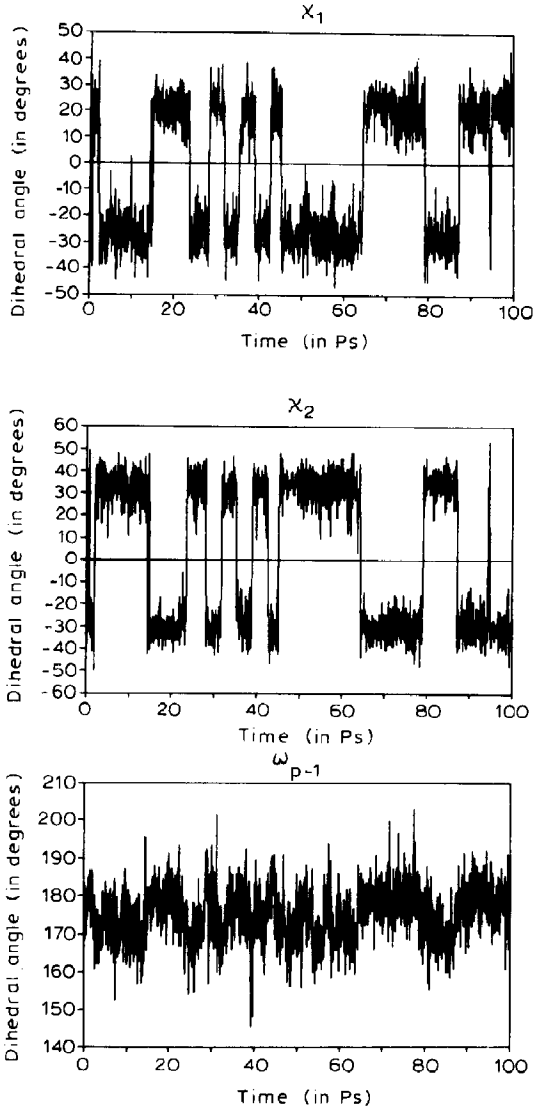

Fig. 5. MD trajectories of the parameters related to the proline conformation.

An analysis of the internal parameters for the 11 structures was carried out: (1) before minimization, (2) after minimization of the structures using SD and CG methods and (3) after NR minimization. The results were analyzed in order to clarify the nature of the helical bend and proline puckering.

The structures obtained after 75–79 ps (set I) of simulation contain proline in the *down* confor-

mation and the structures after 80–85 ps (set II) of simulation have the proline in the *up* conformation. From these studies it is found that χ_1 is always positive and χ_2 is always negative in structures obtained from set I and vice versa in structures from set II. The SD and CG minimization reduces the range of these values drastically and the subsequent NR minimization yields a single set of values of χ_1 and χ_2 ($\chi_1 = 22°$, $\chi_2 = -31.9°$ for set I and $\chi_1 = -32°$, $\chi_2 = 34.9°$ for set II). The trend for other parameters, such as ω_{p-1}, ϕ_{p-1}, ϕ_p and ψ_p, was not clear from the directly simulated structures. These trends become clear in the SD and CG minimized structures with ω_{p-1} taking values from -177.8 to $181.4°$ in set I and from 168.2 to 172.6° in set II. Similarly, ϕ_p assumes values from -58.6 to $-61.4°$ in set I and from -42.6 to $-51.6°$ in set II. ψ_p values range from -37.8 to $-49.0°$ in set I and -49.3 to $-55.6°$ in set II. The NR minimization yields a unique set of values for set I and another unique set of values for set II which are given in table 4. The unique structures thus obtained for sets I and II are plotted in fig. 6. Thus, the proline *up* and *down* structures have two distinct minima which can be characterized by a set of parameters. Apart from the change in the sign of χ_1 and χ_2 values, differences, such as ω_{p-1} deviating more from planarity, ϕ_{p-1} and ψ_p being more negative and ϕ_p being less negative in the *up* structure when compared to the *down* structure are also evident from the average values obtained from MD simulations in the two different regions. These trends are in general agreement with the previously suggested values [7] based on energy minimization of fragments of several crystal structures.

As described in section 3.1.2, the MD simulation studies show that some of the hydrogen bonds, particularly $N_{p+1} \cdots O_{p-3}$ and $N_{p-1} \cdots O_{p-5}$ and virtual torsional angles give an indication as to the nature of bending of the helix. Apart from the normal hydrogen bonds, an additional hydrogen bond between N_{p-3} and O_{p-6} is observed in many structures. The three hydrogen bonds $N_{p+1} \cdots O_{p-3}$, $N_{p-1} \cdots O_{p-5}$ and $N_{p-3} \cdots O_{p-6}$ are

Table 3

Average values (in °) and r.m.s. fluctuations of the parameters related to proline puckering in two different regions, 45–65 and 65–80 ps, during 100 ps MD simulations on Ace-(Ala)$_6$-Pro-(Ala)$_3$-NHMe

Parameters	45–65 ps [a]	65–80 ps [a]
ϕ_{p-1}	−54.1 (±11.2)	−47.5 (±12.5)
ψ_{p-1}	−56.8 (±9.4)	−60.5 (±8.6)
ω_{p-1}	172.5 (±7.3)	178.9 (±6.8)
ϕ_p	−49.5 (±9.6)	−58.8 (±8.5)
ψ_p	−48.9 (±9.0)	−41.6 (±10.9)
χ_1	−23.4 (±15.2)	14.6 (±18.5)
χ_2	28.1 (±18.5)	−22.1 (±22.8)
θ^1_{p-1}	122.3 (±3.2)	123.5 (±3.5)
θ^2_{p-1}	113.4 (±2.9)	114.1 (±3.5)
θ^1_p	122.6 (±2.8)	122.1 (±2.7)
θ^2_p	113.0 (±2.7)	112.1 (±2.9)

[a] Proline residue is in *up* conformation in the region 45–65 ps and in the *down* conformation in the region 65–80 ps.

Table 4

Values (in °) of the dihedral angles for the structures belonging to sets I and II after Newton-Raphson minimization

Dihedral angles	Set I [a]	Set II [a]
ϕ_{p-5}	−47.05	−39.29
ψ_{p-5}	−42.41	−44.72
ω_{p-5}	−179.80	−178.04
ϕ_{p-4}	−57.52	−56.62
ψ_{p-4}	−29.75	−33.00
ω_{p-4}	175.20	175.78
ϕ_{p-3}	−90.50	−91.74
ψ_{p-3}	−48.68	−45.62
ω_{p-3}	−175.83	−175.22
ϕ_{p-2}	−53.71	−55.71
ψ_{p-2}	−47.88	−45.49
ω_{p-2}	−178.70	−179.65
ϕ_{p-1}	−56.15	−59.09
ψ_{p-1}	−63.85	−60.54
ω_{p-1}	178.41	168.28
ϕ_p	−59.99	−44.03
ψ_p	−40.13	−51.87
ω_p	177.43	−178.14
ϕ_{p+1}	−56.10	−56.33
ψ_{p+1}	−49.94	−48.97
ω_{p+1}	178.73	178.83
ϕ_{p+2}	−63.35	−62.90
ψ_{p+2}	−44.58	−44.08
ω_{p+2}	178.12	178.04
χ_1	21.90	−32.10
χ_2	−31.90	35.80

[a] Set I contains structures corresponding to 75.0–79.0 ps in which proline is in the *down* conformation. Set II contains structures corresponding to 80.0–85.0 ps in which proline is in the *up* conformation.

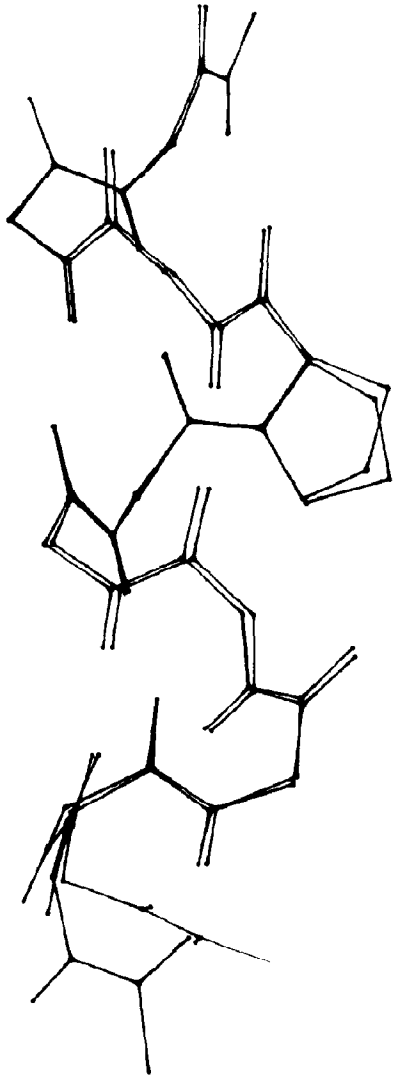

Fig. 6. Plot of minimized structures of Ace-$(Ala)_6$-Pro-$(Ala)_3$-NHMe obtained for proline *up* and *down* conformations.

around an equilibrium value at some time and become weaker at other times. The $N_{p+1} \cdots O_{p-3}$ hydrogen bond in the MD simulated structures of 79, 83, 84 and 85 ps is normal and is very weak in 75, 77, 78, 80, 81 and 82 ps structures. Crystal structure analysis has not revealed this hydrogen bond [8]. Most of the time, minimization of these structures by the SD and CG methods retains this hydrogen bond at approximately the same distance as found before minimization. Further, the $N_{p-1} \cdots O_{p-5}$ hydrogen bond is found to be weak in some of the simulated structures, which was not observed in crystal structure analysis. However, minimization of these structures by SD and CG methods leads to the complete recovery of this hydrogen bond. Another interesting case is the $N_{p-3} \cdots O_{p-6}$ hydrogen bond which is of the $(i \rightarrow i+3)$ type. This hydrogen bond, which was not recognized from crystal structure analysis, is present in some of the MD simulated structures. It is retained by all the structures after minimization by SD and CG methods.

A specific case of Ace-$(Ala)_6$-Pro-$(Ala)_3$-NHMe obtained after 78 ps at different stages of minimization is shown in fig. 7. In the structure before minimization and in that after minimization by SD and CG methods, the hydrogen bond $N_{p+1} \cdots O_{p-3}$ is absent. This hydrogen bond is regained after minimization by the NR method. In both minimized structures, an additional $i \rightarrow i+3$ type of hydrogen bond appears between N_{p-3} and O_{p-6}. In all the structures, the hydrogen bond between the atoms N_p and O_{p-4} is missing due to the lack of an amide proton on N_p.

The values obtained for the virtual torsional angle at different stages of minimization show that VT_3 remains around the standard value ($\simeq 50°$), VT_2 and VT_5 take up a lower value for 75–85 ps and retain this character after SD and CG minimization. VT_4, on the other hand, is correlated with that of the $N_{p+1} \cdots O_{p-3}$ hydrogen bond and is not altered by SD and CG minimization. Thus it appears that the helix fluctuates between an almost straight helix ($H_{p+1} \cdots O_{p-3} \simeq 2.0$ A°; $VT_4 \simeq 50°$) to a bent helix ($H_{p+1} \cdots O_{p-3} \simeq 3.0$ A°; $VT_4 \simeq 70°$) with a period of about 2–5 ps. The NR minimization takes all the structures to a single minimum which corresponds approximately to a straight helix. There can be several reasons for this observation, such as; (a) inherently, the global minimum may be a straight helix with a negligible barrier for bent structures, (b) the size of the segment chosen for the present study may be small from realistic point of view, (c) the environmental effect is not included since the simulation was performed in vacuum and (d) the potential function may not be sensitive enough to

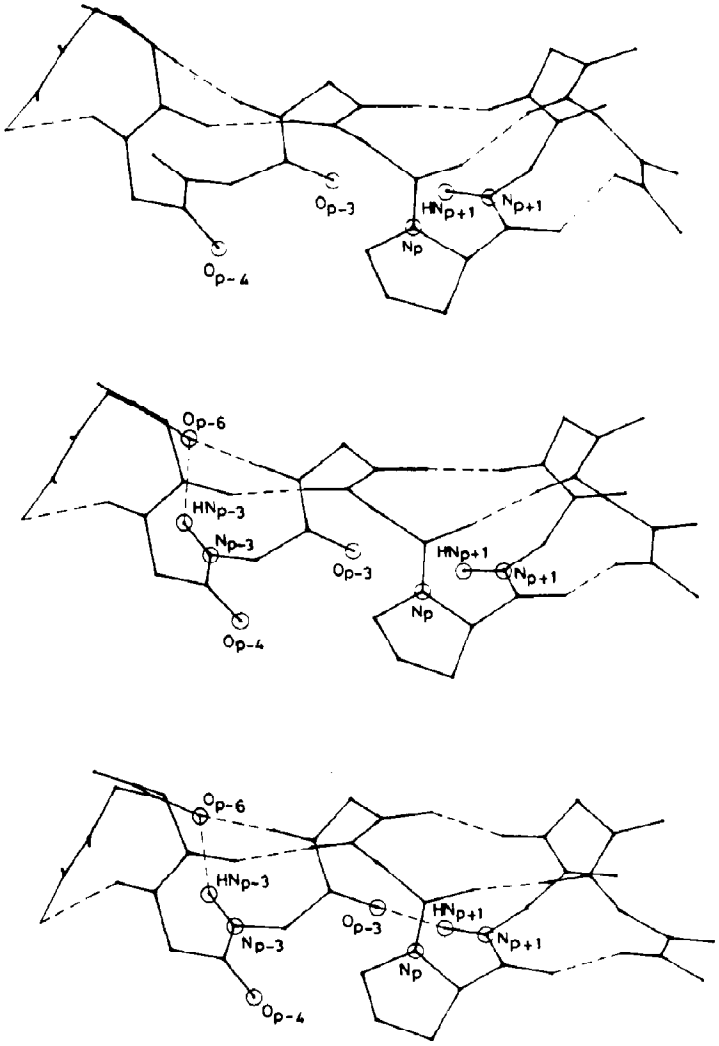

Fig. 7. Plot of Ace-$(Ala)_6$-Pro-$(Ala)_3$-NHMe structure that was obtained after 78 ps of MD simulation. (Top) Before minimization; after minimization by SD and CG methods; (bottom) obtained after minimization by the NR method. See text for details.

distinguish closely related minimum energy structures and these are being investigated further.

4. Conclusions

The MD simulation of Ace-$(Ala)_6$-Pro-$(Ala)_3$-NHMe has been carried out in order to characterize the right-handed α-helix containing a proline residue in the middle.

The studies have yielded the average values and r.m.s. fluctuations of all internal parameters. The deviations obtained in the average values, when compared with an ideal α-helical structure, are consistent with crystal structure analysis. Distinct sets of parameters are obtained for proline *up* and *down* conformations, which were not accessible via crystal structure analysis.

The MD analysis shows that the bend of 20–23° observed in crystal structures of proline-containing helices may be the average of an almost straight helix and a highly bent structure. The period of

oscillation between two extremes is between 2 and 5 ps for the segment chosen for the studies. The proline ring fluctuates between the *up* and *down* conformations with a period of almost 10–20 ps.

The virtual torsional angle VT_4 (ρ) (C^{α}_{p-3}-C^{α}_{p-2}-C^{α}_{p-1}-C^{α}_{p}) and the hydrogen bond N_{p+1}-$H_{p+1} \cdots O_{p-3}$ are correlated with the bend in the helix. The hydrogen bond N_{p-1}-$H_{p-1} \cdots O_{p-5}$ is also affected during MD simulation and an additional $i \rightarrow i+3$ type of hydrogen bond is observed between N_{p-3}-$H_{p-3} \cdots O_{p-6}$.

The energy-minimization studies show that there are clearly two distinct minima for the proline *up* and *down* conformations which are energetically almost equivalent. The energy difference and barrier between different bent structures appear to be small, which allows for frequent interconversion of different bent structures.

References

1 C.B. Anfinsen and H.A. Scheraga, Adv. Protein Chem. 29 (1975) 205.
2 B. Robson and E. Suzuki, J. Mol. Biol. 107 (1976) 327.
3 P.Y. Chou and G.D. Fasman, Biochemistry 13 (1974) 211.
4 J.S. Richardson and D.C. Richardson, Science 240 (1988) 1648.
5 P.R. Schimmel and P.J. Flory, J. Mol. Biol. 34 (1968) 105.
6 L. Piela, G. Nemethy and H.A. Scheraga, Biopolymers 26 (1987) 1587.
7 R. Sankararamakrishnan and S. Vishveshwara, Biopolymers 30 (1990) 287.
8 D.J. Barlow and J.M. Thornton, J. Mol. Biol. 201 (1988) 601.
9 C.J. Brandl and C.M. Deber, Proc. Natl. Acad. Sci. U.S.A. 83 (1986) 917.
10 H.G. Khorana, J. Biol. Chem. 263 (1988) 7439.
11 N.R. Hackett, L.J. Stern, B.H. Chao, K.A. Kronis and H.G. Khorana, J. Biol. Chem. 262 (1987) 9277.
12 T. Mogi, L.J. Stern, B. Chao and H.G. Khorana, J. Biol. Chem. 264 (1989) 14192.
13 P.L. Ahl, L.J. Stern, T. Mogi, H.G. Khorana and K.J. Rothschild, Biochemistry 28 (1989) 10028.
14 K. Gerwert, B. Hess and M. Englehard, FEBS Lett. 261 (1990) 449.
15 K.J. Rothschild, Y.-W. He, D. Gray, P.D. Roepe, S.L. Pelletier, R.S. Brown and J. Herzfeld, Proc. Natl. Acad. Sci. U.S.A. 86 (1989) 9832.
16 R. Bazzo, M.J. Tappin, A. Pastore, T.S. Harvey, J.A. Carver and I.D. Campbell, Eur. J. Biochem. 173 (1988) 139.
17 P. Weiner and P.A. Kollman, J. Comput. Chem. 2 (1981) 287.
18 P.K. Weiner, U.C. Singh, P.A. Kollman, J. Caldwell and D.A. Case, A Molecular mechanics and dynamics program — AMBER (University of California, San Francisco). Ref. 17 describes the program.
19 S.J. Weiner, P.A. Kollman, D.A. Case, U.C. Singh, C. Ghio, G. Alagona, S. Profeta Jr and P. Weiner, J. Am. Chem. Soc. 106 (1984) 765.
20 S.J. Weiner, P.A. Kollman, D.J. Nguyen and D.A. Case, J. Comput. Chem. 7 (1986) 230.
21 H.J.C. Berendsen, J.P.M. Postma, W.F. Van Gunsteren, A. DiNola and J.R. Haak, J. Comput. Phys. 81 (1984) 3684.
22 S. Arnot and A.J. Wonacott, J. Mol. Biol. 21 (1966) 371.
23 L.G. Presta and G.D. Rose, Science 240 (1988) 1632.
24 F. Colonna-Cesari, S. Premilat, F. Heitz, G. Spach and B. Lotz, Macromolecules 10 (1977) 1284.
25 R. Sankararamakrishnan and S. Vishveshwara, J. Biomol. Struct. Dyn. 7 (1989) 187.